Available online at www.sciencedirect.com
SCIENCE DIRECT®
Polymer 44 (2003) 7971–7978
polymer
www.elsevier.com/locate/polymer

Effects of droplet size on photorefractive properties of polymer dispersed liquid crystals

Hiroshi Ono[a,*], Hirohito Shimokawa[a], Akira Emoto[a], Nobuhiro Kawatsuki[b]

[a]*Department of Electrical Engineering, Nagaoka University of Technology, 1603-1 Kamitomioka, Nagaoka 940-2188, Japan*
[b]*Department of Materials Science and Chemistry, Himeji Institute of Technology, 2167 Shosha, Himeji 671-2201, Japan*

Received 7 July 2003; received in revised form 14 October 2003; accepted 16 October 2003

Abstract

Effects of liquid-crystal droplet size on orientational photorefractive properties of the polymer dispersed liquid crystals are investigated experimentally. The composites consist of the same chemical components, but the liquid crystal droplet size was varied by controlling the fabrication process. Particular attention is given to the observation and qualitative and/or quantitative modeling of the resolution, dependence of the applied dc field, dynamics of grating generation and photocurrents, which is strongly dependent on the liquid crystal droplet size.

PACS: 42.65.Hw; 42.70.Df; 42.70.Nq

Keywords: Polymer dispersed liquid crystal; Hologram; Droplet size

1. Introduction

In recent years, the expectation for various types of real-time holographic gratings has grown in applications ranging from light controlling in photonic systems. From the point of view of photonics, organic materials possess some important advantages over the inorganics. Several types of photosensitive organic materials have been developed into new active devices, including photochromic [1–6] and photorefractive materials [7–32]. Among organic photorefractive materials including organic crystal, polymer composites and liquid crystal, photorefractive liquid crystals have several advantages in comparison with other materials: a low operating voltage, which is required for its application to photorefractive material in order to realize wave mixing, a large refractive index modulation resulting from the large anisotropy of the mesogenic molecules, and ease of fabrication, developed in the display industry [19]. Low-molar-mass nematic liquid crystals show high-performance photorefractivities by giving photoconductivity to the liquid crystals. However, since the discovery of photorefractive low-molar-mass liquid crystals, good photorefractive performance has been observed only for large fringe spacing [7–13,21–23,25–32].

Recently, it has been found that the performance of photorefractive liquid crystal is improved by combining low-molar-mass liquid crystal with a polymer and photorefractive Bragg gratings can be recorded in such materials [14–20,24]. Polymer dispersed liquid crystals (PDLCs) have been studied in a different research field for their potential in flexible displays and architectural applications [33]. They can be switched from a scattering state to a transparent state by application of an appropriate electric field. Application of an electric field makes the director of the liquid crystal droplets in the polymer binder align parallel to the field. According to numerous studies about the switching characteristics of the PDLCs, it is well known that the switching response depends on the morphology of the PDLCs. Although the performance of the photorefractive liquid crystal is improved by combining low-molar-mass liquid crystal with a polymer, the properties are expected to be strongly dependent on the morphology of the PDLCs. In order to clarify the reason why the photorefractive performance is improved by combining low-molar-mass liquid crystal with polymer, it is very important to investigate the effects of the morphology on the photorefractive properties of the PDLCs. In the present paper, we extensively investigated the grating formation speed and resolution, as well as their dependence on the morphology of photorefractive PDLCs. The main goal of this article is to

* Corresponding author. Tel.: +81-258-47-9528; fax: +81-258-47-9500.
E-mail address: onoh@nagaokaut.ac.jp (H. Ono).

0032-3861/$ - see front matter © 2003 Elsevier Ltd. All rights reserved.
doi:10.1016/j.polymer.2003.10.038

report the observation of the grating formation, and of the photocurrent in the photorefractive PDLCs with different liquid crystal droplet size.

2. Experiment

2.1. Materials

In the present paper, the photorefractive PDLCs were prepared by thermally-driven phase separation processes. In a thermally-induced phase separation process, a thermoplastic polymer is heated into a melt and mixed with a low-molar-mass liquid crystal to form single phase solution. The liquid-crystal phase separates into droplets as the system is cooled back to room temperature, forming the PDLC film. The droplet size can be varied by the rate of cooling, with rapid cooling leading to smaller droplet sizes, which is preferable to investigate the effects of the droplets size on the photorefractive properties. We investigated the photorefractive properties of two samples with different liquid crystal droplet sizes. These composites consist of the same chemical components, but one contains small sizes of liquid crystal droplets (S-PDLC) and another one large sizes of droplets (L-PDLC). The photorefractive PDLC contains poly(methyl methacrylate) (PMMA) as the thermoplastic polymer. The PMMA was commercially available and obtained from Tokyo Kasei Organic Chemicals. A nematic low-molar-mass liquid crystalline mixture named E7 was obtained from BDH-Merck, Japan. Fullerene (C_{60}), which has been already reported as the photoconductive sensitizer for mesogenic materials, was obtained from Tokyo Kasei Organic Chemicals. The composition (PMMA:E7) of our samples was controlled to be 5:95, 10:90, and 15:85. The content of dopant (C_{60}) was $\sim$0.05 wt% for all samples. Photorefractive PDLC samples were prepared by mixing the components at 150 °C and stirring until a homogeneous solution was obtained. At the same temperature, the resulting homogeneous solution was sandwiched between two indium tin oxide (ITO) coated-glass substrates with a 10-μm-thick polyester film as a spacer. Usually, when the polymer that exhibits no liquid crystal phase, such as PMMA, is mixed with nematic low-molar-mass liquid crystal, phase separation occurs. When the mixture containing PMMA cooled down, the phase separation occurs and the resulting PDLC film scatters light. As studied in a different research field for their potential in displays, the light scattering results from the mismatch between the refractive index of E7 and that of the PMMA binder. Application of an electric field across the PDLC film makes the director of the droplets align parallel to the field. Since the ordinary refractive index of E7 is nearly matched with that of the PMMA binder, the film becomes transparent. The liquid crystal droplet size was varied by the rate of cooling. The rapid cooling in the air leads to smaller droplets (S-PDLC), while the slow cooling of about 0.4 K/min in the programmable oven leads to larger droplets (L-PDLC). The morphology of the composite films was observed by a polarization microscope. Fig. 1(a)–(f) shows the photographs of S-PDLC and L-PDLC samples on varying the composition. It was clearly observed that the liquid crystal domain sizes in the S-PDLC samples were smaller than those in the L-PDLC samples.

2.2. Measurements

The photorefractive gratings were written using two linearly polarized, mutually coherent He–Ne laser beams, which emits cw 633 nm light, with an intensity of 5.0 mW each. A linearly polarized beam from a continuous-wave He–Ne laser was divided into two beams of equal intensity by a beam splitter. Two coherent *p*-polarized beams were superposed onto the sample on the same 510-μm-diam spot, which was measured by a scanning method (Photon, Inc.: Beam Scan Model 1080). We employed a tilted geometry configuration in which the two beams intersected in the

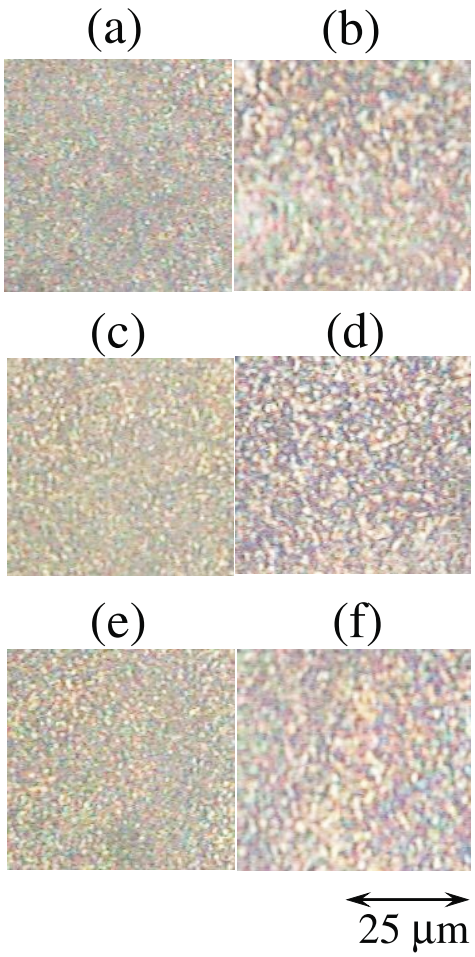

Fig. 1. Polarizing optical microscopic photographs for the PDLC samples. The polymer concentrations were (a) and (b) 5 wt%, (c) and (d) 10 wt%, and (e) and (f) 15 wt%. The samples (a), (c) and (e) were prepared by the rapid cooling process (S-PDLCs) and samples (b), (d) and (f) by the slow cooling process (L-PDLCs).

material at a tilted angle of 45° with respect to the sample normal. The fringe spacing was varied by controlling the incident angle between the two writing beams. The dc electric field was applied by a dc power supply (Hewlett–Packard: E3612A) through two ITO coated-glass substrates. It is necessary to determine whether the grating is a thin (Raman-Nath) or volume (Bragg) grating. For this purpose, the following well-known parameter can be used [34].

$$Q = \frac{2\pi d\lambda}{\Lambda^2 n} \tag{1}$$

where λ is the wavelength of the light, n is the index of refraction, d is the thickness of the grating, and Λ is the grating constant. Under our experimental conditions, the grating constants were varied between about 10 and 50 μm. Judging from the value of the parameter $Q \ll 1.0$ under our experimental conditions, we deal with a thin grating case e.g. a Raman-Nath diffraction for which the directions of m-th diffraction orders are given by $\theta_m = \arcsin(m\lambda/\Lambda)$. For the Raman-Nath regime of optical diffraction, the angular spread of the grating vector is much larger than the Bragg diffraction angle, and multiple orders of diffraction are therefore, allowed. Since the writing beams are self-diffracted in the Raman-Nath regime, characterization of the generated gratings can be performed without using another beam as a probe. The transient signal for the photorefractive grating generation was measured by monitoring the beam intensities of the first-order self-diffraction beam using a monitoring system composed of a silicon photodiode, a Kikusui K-7101A digitizing oscilloscope, and a personal computer. All measurements were performed at 20 °C.

3. Results and discussion

Since the diffraction is of the Raman-Nath type under our experimental conditions, a self-diffraction process was effective at certain value of dc voltage applied to the PDLC samples and a result of it, in a far field after the sample, the first order diffraction spots appeared. Higher order diffraction was almost invisible in the samples studied. The photorefractive effect refers to spatial modulation of the refractive index $[\Delta n(x,y)]$ by a specific mechanism: light-induced charge distribution. The effect arises when charge carriers, photogenerated by a spatially modulated light intensity, separate by drift and diffusion processes and become trapped to produce a nonuniform space-charge distribution. The resulting space charge field reorients the liquid crystalline molecules and modulates the refractive index to generate a nonlocal phase grating. The refractive index modulation due to a nonlocal phase grating is written as

$$\Delta n(x,y) = n_2 I\left(x + \frac{\phi_p}{2\pi}\Lambda, y\right), \tag{2}$$

where ϕ_p is the spatial phase shift between the interference light and refractive index modulation and n_2 is a real number. The intensity-dependent (nonlinear) phase is given by

$$\phi(x,y) = kd\Delta n(x,y). \tag{3}$$

The nonlocal phase grating is conducted to formulate diffraction efficiencies which pass through the nonlocal phase grating. The diffraction pattern is

$$I_{dif}(x',y') = |\xi_1(x',y') + \xi_2(x',y')|^2, \tag{4}$$

where

$$\xi_1(x',y') = E_1 \int\int \exp(ikx\theta)\exp[i\phi(x,y)] \exp\left[-i\frac{k}{R}(xx' + yy')\right]dxdy, \tag{5}$$

$$\xi_2(x',y') = E_2 \int\int \exp(-ikx\theta)\exp[i\phi(x,y)] \exp\left[-i\frac{k}{R}(xx' + yy')\right]dxdy \tag{6}$$

where R is distance between the sample and a screen, E_1, E_2 are the wave amplitudes, k is the wavenumber and 2θ is the crossing angle between the two beams. The intensities of the positive order diffraction beams from the photorefractive PDLCs were larger than those of the negative order diffraction beams. According to Eqs. (5) and (6), the anti-symmetric diffraction pattern is a result of photorefractive-like nonlocal gratings generated in the PDLC samples.

The refractive index changes versus the applied dc field are plotted in Fig. 2. At the beginning of the curves a general trend of larger refractive index change can be observed with increasing the applied dc electric fields. No diffraction was observed for all samples when the applied dc field was zero. There is an apparent threshold and saturation at certain value of the applied dc field, a voltage beyond which refractive index change decreases. The maximum value of the refractive index change increases with increasing the polymer concentration although the higher applied dc field is necessary. In addition, the higher value of the applied dc field to obtain the maximum refractive index change in the S-PDLCs is necessary in comparison with the L-PDLCs. The internal electric field strength within a PDLC layer is a result of a static field applied sample and spatially modulated field. In order to prove that the self-diffraction resulted from the presence of a space-charge field (E_{SC}) Rudenko and Sukhov investigated the mechanism of the photoconductivity in the liquid crystals [7,8]. They observed that the dependence of the conductivity σ in dye-doped low-molar-mass liquid crystals on light intensity I is $(\sigma - \sigma_d) \propto \sqrt{I}$, where the subscript d specifies the dark conductivity, and the dependence of the conductivity on the concentration of the dye did not have a percolation limit at low dye concentration. They concluded that the conductivity was of an

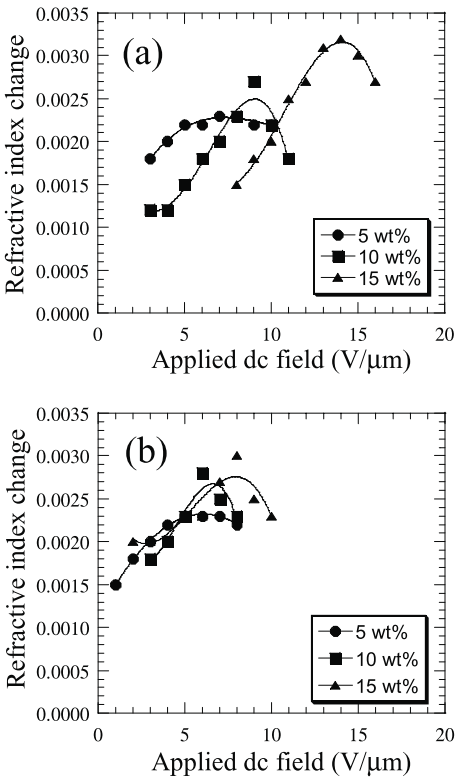

Fig. 2. Refractive index change on (a) S-PDLC and (b) L-PDLC samples on varying the applied dc field. Polymer concentration was set to be 5 (circles), 10 (squares), and 15 wt% (triangles).

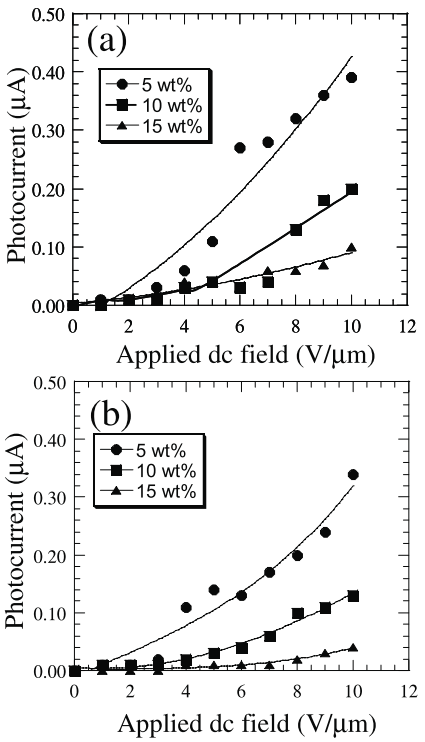

Fig. 3. Photocurrent as a function of the applied dc field for (a) S-PDLC and (b) L-PDLC samples under 5.0 mW beam power illumination (beam diameter 1.2 mm). Polymer concentration was set to be 5 (circles), 10 (squares), and 15 wt% (triangles).

ion drift nature and the only process of importance that prevents ions from forming a space charge was the actual quadratic recombination of these ions. Thus the mechanism of light induced space charge field formation is deeply linked with ion conduction and photoconduction in photorefractive PDLC films. Fig. 3 shows the photocurrent for S-PDLC (Fig. 3(a)) and L-PDLC (Fig. 3(b)) samples as a function of the applied dc field. The photocurrent was calculated as the difference between the total current through the illuminated sample and dark current. The sample was illuminated by a 5.0 mW, 633 nm beam with a 1.2 mm diameter. One point to be noted is that the value of photoconduction was decreased with increasing the polymer contents for both S-PDLC and L-PDLC samples. We attribute the behavior to a small amount of polymer wall which exists in the PDLC sample, in which polymer and low-molar-mass liquid crystal are phase separated. The photoconductive effect originates in the ion conduction in the liquid crystal/polymer composites and is associated with an influence of the morphology of the composites, i.e. the interfaces between the low-molar-mass liquid crystal droplet and polymer. The domain size of the liquid crystal droplets is much smaller than the grating constant as shown in Fig. 1 and the photoexcited ions have to migrate beyond the polymer wall because the polymer and low-molar-mass liquid crystal are phase-separated. It is easy to understand that total length for the photoexcited ions to migrate beyond the polymer wall increases with increasing the polymer contents and the photocurrent at the same applied dc field decreased with increasing the polymer contents. Another point to be noted is that there are little discrepancies between the experimental results for S-PDLCs and those for L-PDLCs. This means that the conduction properties of the photoexcited ions are strongly associated with an influence of the total thickness of the polymer wall, which is more at a more polymer concentration and is not affected by the liquid crystal droplet size. Thus, since the photorefractive properties as shown in Fig. 2 are strongly dependent on the droplet size in the PDLCs, while the photocurrent properties as shown in Fig. 3 are scarcely affected by the liquid crystal droplet size, the effects of the droplet size on the photorefractive properties cannot be explained by the ion conduction processes in the PDLCs.

One has to notice that there is another possibility to explain the above-mentioned effects of the droplet size on the photorefractive properties in the PDLC film. In the PDLC samples, it is well-known that small liquid crystal domains produce higher voltages for electrical switching by increasing the free energy of elastic deformations within the liquid crystal [33]. In order to clarify that the mechanism is linked with electric field driven reorientation of nematic director in the droplets, the transient signal for the photorefractive grating generation was measured by monitoring the beam intensities of the first-order self-diffraction beam. A typical grating buildup dynamics in photorefractive PDLC

films is shown in Fig. 4. First, in order to estimate the rise time of the induced photorefractive gratings, we tried experimental data with the monotonic exponential as follows:

$$\eta(t) = 1 - \exp\left(-\frac{t}{\tau}\right). \tag{7}$$

Since the appropriate solution could not be obtained, we tried to fit the experimental data with the following equation:

$$\eta(t) = 1 - A_{\text{fast}} \exp\left(-\frac{t}{\tau_{\text{fast}}}\right) - A_{\text{slow}} \exp\left(-\frac{t}{\tau_{\text{slow}}}\right). \tag{8}$$

The theoretical fitting curve calculated from Eq. (8) is in good agreement with the experimental data as shown in Fig. 4 and one can clearly identify a transient buildup superposed to the double exponential growth of the grating. This clearly indicates that there are two different reorientation processes in the photorefractive PDLC films. According to the past study about the electrooptic effects in PDLC, the PDLC shows such combinations of time scales for the reorientation of the liquid crystal molecules in the bulk of the droplet and at the surface of the droplet [33]. According to the two-stage rise model for the PDLC films, upon application of an electric field, the nematic near the center of the droplet quickly reorients with the field, giving a fast response, and the surface layer and defect structure then rotate with a slower response. Although it is not easy to completely understand reorientation processes under the space charge field because of the complicated morphology of the PDLC, it is not unnatural to consider that τ_{fast} and τ_{slow} correspond to reorientation speed in the bulk of the liquid crystal droplet and that at the surface of the droplet. The observed time ranges of 0.1–2.0 s, which seems to be slower than the response time of the conventional PDLC reported so far [33], usually less than about 10 ms.

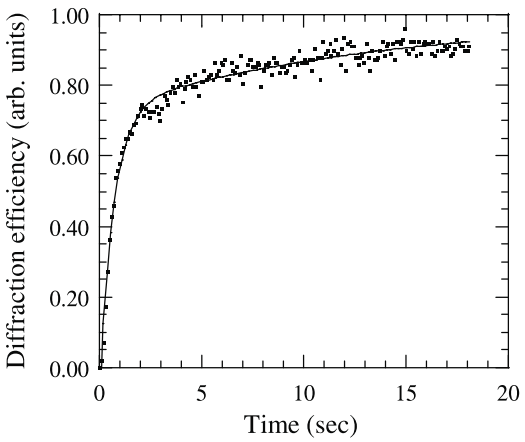

Fig. 4. The typical grating buildup dynamics in the photorefractive S-PDLC samples induced by the interference of two 633 nm beams. Dotted circles were obtained from experimental observation and solid curves from theoretical fitting. The polymer concentration was 10 wt% and the grating constant 20 μm. The dc field applied to the S-PDLC sample was 8.0 V/μm.

However, one has to notice that the reorientation speed is strongly dependent on the value of the electric field [33]. We already estimated the space-charge field in the photorefractive liquid crystal-polymer dispersions [35]. The value of the space-charge field is around 0.1 V/μm and this value is much smaller than that usually applied to the conventional PDLC.

Figs. 5–7 summarize the parameters used in Eq. (8) as a function of applied dc field. As in the case of reorientation fields, the dynamic response of a nematic droplet depends on the relative strength of the electric field and elastic forces acting on the nematic, which drives the droplet reorientation. Viscous torques resist the reorientation, showing the dynamics of the process. These factors are affected by the dielectric, elastic, and viscosity properties of the nematic, as well as the morphology of the nematic droplets and polymer network. For reorientation by an electric field, it is convenient to discuss film dynamics in terms of electric (Γ_e), elastic (Γ_d), and viscous torques (Γ_v). Response time is determined by balancing all torques: $\Gamma_d + \Gamma_e + \Gamma_v = 0$, and rise time constant have been represented by [36]

$$\tau_{\text{rise}} \approx \frac{\gamma}{\Delta\varepsilon E_a^2 - \dfrac{K(l^2-1)}{a^2}}, \tag{9}$$

where γ is a rotational viscosity coefficient, $\Delta\varepsilon$ is the dielectric anisotropy, K is some elastic constant and E_a is the magnitude of the electric field within the liquid crystal. For the case of an ellipsoidal droplet elongated along the

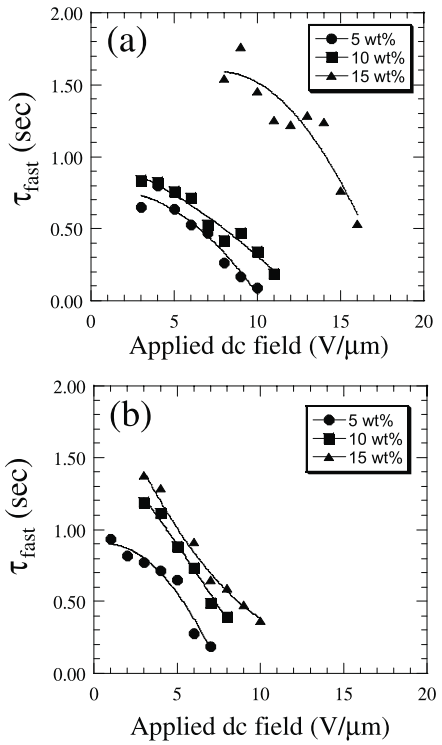

Fig. 5. The first component of grating formation response versus applied dc field for (a) S-PDLC and (b) L-PDLC samples. Polymer concentration was set to be 5 (circles), 10 (squares), and 15 wt% (triangles).

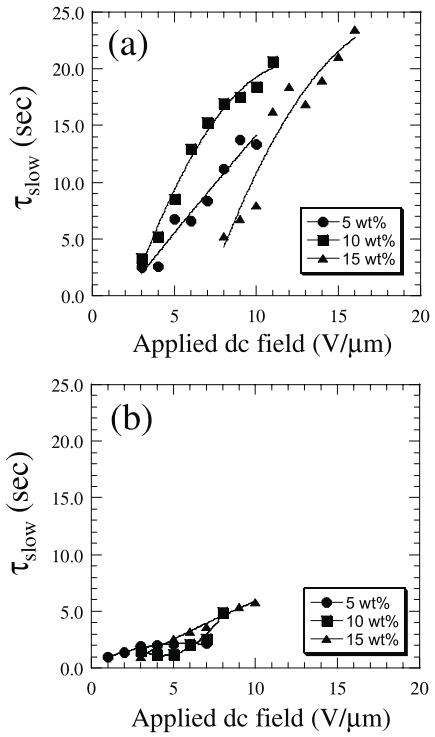

Fig. 6. The slow component of grating formation response versus applied dc field for (a) S-PDLC and (b) L-PDLC samples. Polymer concentration was set to be 5 (circles), 10 (squares), and 15 wt% (triangles).

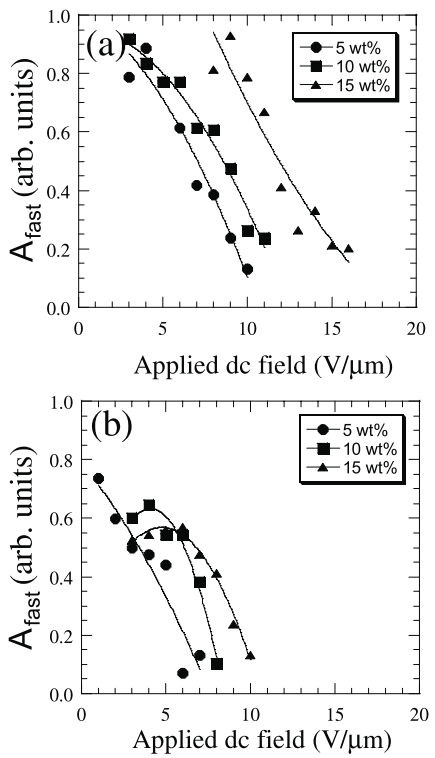

Fig. 7. The amplitude of the fast component of grating formation response versus applied dc field for (a) S-PDLC and (b) L-PDLC samples. The total amplitude of the response is normalized to unity. Polymer concentration was set to be 5 (circles), 10 (squares), and 15 wt% (triangles).

film plane, major semi-axis length is a and minor semi-axis length b, which define an aspect ratio $l = a/b$ (shape anisotropy). Similarly, the rise time is predicted to scale as following another expression [37,38]:

$$\tau_{\text{rise}} \approx \frac{\gamma}{\varepsilon_0 \Delta\varepsilon (E_a^2 - E_{\text{th}}^2)}, \tag{10}$$

where E_{th} is the threshold voltage for reorienting a droplet. The response time became slow with increasing the polymer concentration and was strongly dependent on the applied dc field as shown in Figs. 5 and 6. Eq. (10) shows that the response time and threshold voltage are closely related. It is known that the reorientation field scales inversely with droplet size because the small liquid crystal domains produce the high free energy of elastic deformations within the liquid crystal. It is also known that higher polymer concentrations usually produce smaller liquid crystal domains, which produce higher voltages. These considerations about effects of polymer concentrations and droplet sizes are consistent with the experimental results described in Fig. 2. Considering both the experimental results described in Fig. 2 and Eq. (10), the faster response time should be obtained for the photorefractive PDLCs with lower polymer concentrations and/or smaller liquid crystal domains. Indeed, this phenomenon was experimentally demonstrated in both S-PDLCs and L-PDLCs as shown in Figs. 5 and 6. According to Eq. (9) or Eq. (10), strong fields applied to a droplet have to induce a faster reorientation than small fields. A general trend of faster τ_{fast} can be observed with increasing the applied dc electric fields as shown in Fig. 5, while τ_{slow} became slow as shown in Fig. 6. In order to explain this phenomenon one has to extensively consider the two-stage response for PDLCs. As above-mentioned in the present article, according to the two-stage rise model for the PDLC films, upon application of an electric field, the nematic near the center of the droplet quickly reorients with the field, giving a fast response, and the surface layer and defect structure then rotate with a slower response. Since, under the low electric field, the surface layer is a small fraction of the total volume of the droplet, this response is smaller in magnitude than the fast rise response. As increasing the electric field, the surface layer spreads to the interface between the liquid crystal and polymer and this response should become large in magnitude. Indeed, this model is also consistent with the rise amplitude in magnitude ratio exhibited in Fig. 7.

The calculated refractive index change estimated from the measured diffraction efficiencies as functions of the period of the interference pattern is shown in Fig. 8. The maximum response is obtained for a grating period about 25–30 μm in the case of the S-PDLC samples, while that is obtained for 20–25 μm in the case of the L-PDLC samples, which is dependent on the polymer concentration and the grating period for the maximum response seems to be increased with increasing the polymer concentration. In any way, higher polymer concentrations usually produce

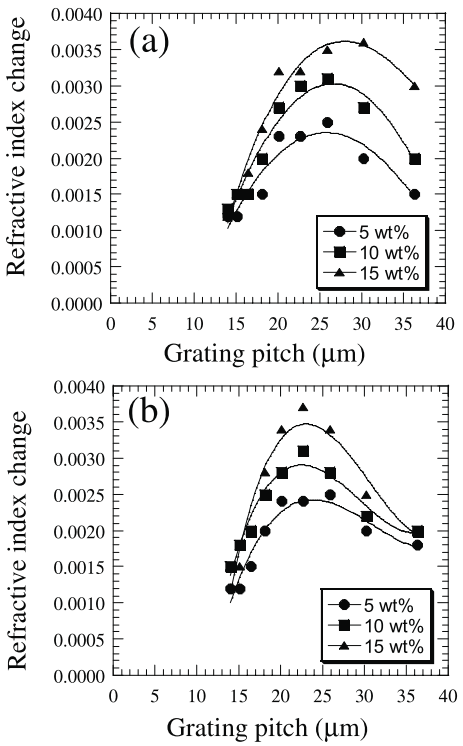

Fig. 8. Refractive index change in (a) S-PDLC and (b) L-PDLC samples on varying the grating spacing. Polymer concentration was set to be 5 (circles), 10 (squares), and 15 wt% (triangles).

smaller liquid crystal domains and the smaller liquid crystal domains give the longer grating period for the maximum response. The intermolecular elastic torques associated with director axis reorientation and torques exerted by the space-charge fields are dependent on the grating spacing. The relationship between the periodic space-charge field and the resulting refractive index modulation can be roughly estimated by means of elastic continuum theory, as has been already reported by others [12]. According to the previous study, the space charge field is proportional to q and the elastic restoring force varies as $\pi^2 d^{-2} + q^2$. The resulting induced director reorientation angle is proportional to $q/(\pi^2 d^{-2} + q^2)$, which has a maximum at $q \sim \pi/d$, or a grating constant $\Lambda_{max} \approx 2d$. In the present study, for $d = 10\ \mu$m, $\Lambda_{max} = 20\ \mu$m. It is known that this theory can well-explain effects of the grating period on the photorefractive properties in the photorefractive low-molar-mass liquid crystals. However the discrepancy between the experimental and theoretical value cannot be ignored in the case of the PDLC samples and the larger Λ_{max} is clearly observed for the photorefractive PDLCs as shown in Fig. 8. We attribute this phenomenon to the phase-separated morphology. The continuum theory might be invalid in the case of PDLC films because of the phase-separation in the PDLC. According to the past studies of the PDLC, the restoring force is related to the liquid crystal domain size. For each different liquid crystal domain size for S-PDLCs and L-PDLCs, in which the liquid crystal domain size is also dependent on the polymer concentration, the restoring force and the resulting Λ_{max} will vary. Since smaller liquid crystal domains will produce the larger restoring force, the smaller droplet should produce larger restoring force and resulting longer Λ_{max}. This model is also consistent with the experimental results exhibited in Fig. 8. Furthermore one has to notice another feature appeared in experimental data described in Fig. 8. The experimental data for the photorefractive PDLCs give broader peak in comparison with those for the photorefractive low-molar-mass liquid crystals presented in past study. The mechanism of this phenomenon is linked with distribution of the liquid crystal domain size. The restoring force is dependent on the liquid crystal domain size and broad peak in experimental data described in Fig. 8 could be obtained.

4. Summary

In this article, we have presented the results of some experimental studies aimed at quantifying the photorefractive response of the photorefractive polymer dispersed liquid crystals with different sizes of liquid crystal domain, and their dynamics. We extensively investigated the grating formation speed, resolution, and photocurrent, as well as their dependence on the droplet sizes of the photorefractive polymer dispersed liquid crystals. The mechanism is linked with electric field driven reorientation of nematic director in the droplets and the photorefractive response is explained by the theory considering the relative strength of the electric field and elastic forces acting on the nematic, which drives the droplet reorientation.

Acknowledgements

We thank Tokuyama Science Foundation for supporting our study. This work was partially supported by a Grant-in-aid for Scientific Research from the Ministry of Education, Science and Culture of Japan.

References

[1] Ichimura K. Chem Rev 2000;100:1847.
[2] Frey L, Kaczmarek M, Jonathan JM, Goosen G. Opt Mater 2001;18:91.
[3] Simonov AN, Larichev AV, Shibaev VP, Stakhanov AI. Opt Commun 2001;197:175.
[4] Serak S, Kovalev A, Agashkov A, Gleeson HF, Watson SJ, Reshetnyak V, Yaroshchuk O. Opt Commun 2001;187:235.
[5] Matczyszyn K, Bartkiewicz S, Sahraoui B. Opt Mater 2002;20:57.
[6] Wang YJ, Pei M, Garlisle GO. Opt Lett 2003;28:840.
[7] Rudenko EV, Sukhov AV. JETP Lett 1994;78:143.
[8] Rudenko EV, Sukhov AV. JETP Lett 1994;78:875.
[9] Khoo IC, Li H, Liang Y. Opt Lett 1994;19:1723.
[10] Khoo IC. Opt Lett 1995;20:2137.

[11] Wiederrecht GP, Yoon BA, Wasielewski MR. Science 1994;270: 1794.
[12] Khoo IC. Liquid crystals. New York: Wiley; 1995.
[13] Wiederrecht GP, Yoon BA, Svec WA, Wasielewski MR. J Am Chem Soc 1997;119:3358.
[14] Ono H, Kawatsuki N. Opt Lett 1997;22:1144.
[15] Golemme A, Volodin BL, Kippelen B, Peyghambarian N. Opt Lett 1997;22:1226.
[16] Wiederrecht GP, Wasielewski MR. J Am Chem Soc 1998;120:3231.
[17] Ono H, Saito I, Kawatsuki N. Appl Phys Lett 1998;72:1942.
[18] Golemme A, Kippelen B, Peyghambarian N. Chem Phys Lett 2000; 319:655.
[19] Wiederrecht GP. Annu Rev Mater Res 2001;31:139.
[20] Bai Y, Chen X, Wan X, Zhou QF, Liu H, Zhang B, Gong Q. Appl Phys B 2001;73:35.
[21] Lee W, Yeh SL. Appl Phys Lett 2001;79:4488.
[22] Fuller MJ, Wasielewski MR. J Phys Chem B 2001;105:7216.
[23] Pagliusi P, Cipparrone G. Appl Phys Lett 2002;80:168.
[24] Bai Y, Chen X, Wan X, Zhou Q, Li H, Zhang B, Gong Q. Appl Phys Lett 2002;80:10.
[25] Lee W, Chen HY, Yeh SL. Opt Exp 2002;10:482.
[26] Kamania N, Putilin S, Stasel'ko D. Synth Met 2002;127:129.
[27] Lee W, Wang YL. J Phys D: Appl Phys 2002;35:850.
[28] Termine R, Golemme A. J Phys Chem B 2002;106:4105.
[29] Klysubun P, Indebetouw G. J Appl Phys 2002;91:897.
[30] Kim HD, Jung S, Yoon CS, Kim JD. Appl Phys B 2002;75:123.
[31] Kim HE, Min W, Jung S, Yoon GS, Kim JD. Jpn J Appl Phys 2003;42: L44.
[32] Khoo IC, Ding J, Zhang Y, Chen K, Diaz A. Appl Phys Lett 2003;82: 3587.
[33] Drzaic PS. Liquid crystal dispersions. Singapore: World Scientific; 1995.
[34] Kogelnik H. Bell Syst Tech J 1969;48:2909.
[35] Ono H, Kawamura T, Frias NM, Kitamura K, Kawatsuki N, Norisada H. Appl Phys Lett 1999;75:3632.
[36] Wu BG, Erdmann JH, Doan JW. Liq Cryst 1989;5:1453.
[37] Drzaic PS. Liq Cryst 1988;3:1543.
[38] Adomenas A, Buivydas M, ereikis A, Pamedityte V. Mol Cryst Liq Cryst 1992;215:153.